FERMILAB-PUB-22-272-DI-ND-PPD

Prepared for submission to JINST

Qualification study of SiPMs on a large scale for the CMVD Experiment

Mamta Jangra,[a,b,1] Raj Bhupen,[a,b] Gobinda Majumder,[b] Kiran Gothe,[b] Mandar Saraf,[b] Nandkishor Parmar,[b] B. Satyanarayana,[b] R.R. Shinde,[b] Shobha K. Rao,[b] Suresh S Upadhya,[b] Vivek M Datar,[c] Douglas A. Glenzinski,[d] Alan Bross,[d] Anna Pla-Dalmau,[d] Vishnu V. Zutshi,[e] Robert Craig Group,[f] and E Craig Dukes,[f]

[a] *Homi Bhabha National Institute, Mumbai-400094, India*
[b] *Tata Institute of Fundamental Research, Mumbai-400005, India*
[c] *The Institute of Mathematical Sciences, Chennai-600113, India*
[d] *Fermi National Accelerator Laboratory, IL 60510, United States*
[e] *Northern Illinois University, IL 60510, United States*
[f] *Virginia University, VA, United States*

E-mail: mamta.jangra@tifr.res.in

Abstract: A Cosmic Muon Veto (CMV) detector using extruded plastic scintillators is being designed around the mini-Iron Calorimeter (mini-ICAL) detector at the transit campus of the India based Neutrino Observatory, Madurai for the feasibility study of shallow depth underground experiments. The scintillation signals that are produced in the plastic due to muon trajectories are absorbed by wavelength shifting (WLS) fibres. The WLS fibres re-emit photons of longer wavelengths and propagate those to silicon photo-multipliers (SiPMs). The SiPMs detect these photons, producing electronic signals. The CMV detector will use more than 700 scintillators to cover the mini-ICAL detector and will require around 3000 SiPMs. The design goal for the cosmic muon veto efficiency of the CMV is >99.99%. Hence, every SiPM used in the detector needs to be tested and characterised to satisfy the design goal of CMV. A mass testing system was developed for the measurement of gain and choice of the overvoltage (V_{ov}) of each SiPMs using an LED driver. The V_{ov} is obtained by studying the noise rate, the gain of the SiPM. This paper describes the experimental setup used to test the SiPMs characteristics along with detailed studies of those characteristics as a function of temperature.

Keywords: SiPM, Cosmic Muon Veto, Calibration, Noise

arXiv:2203.16963v1 [physics.ins-det] 31 Mar 2022

[1] Corresponding author.

This manuscript has been authored by Fermi Research Alliance, LLC under Contract No. DE-AC02-07CH11359 with the U.S. Department of Energy, Office of Science, Office of High Energy Physics.

Contents

1 Introduction

A 51 kton magnetized Iron Calorimeter (ICAL) was proposed [1] at the underground laboratory of the India-based Neutrino Observatory (INO) to precisely measure the parameters of atmospheric neutrinos, mainly to study the effect of matter on neutrino oscillations [2]. The underground laboratory (with a rock cover of more than 1 km in all directions) along with ICAL is planned to be located in Bodi West hills at Theni ($9^{\circ}57'50.1''$ N, $77^{\circ}16'21.8''$ E), India. ICAL will consist of three modules, where each of the modules will contain 150 layers of Resistive Plate Chambers (RPCs) interfaced between 5.6 cm thick iron plates. Due to the low interaction cross-section of neutrino, there are only a handful of neutrino events in a day whereas there are a large number of cosmic-ray muons $\sim 3 \times 10^8$ /day incident on the surface about a km above the proposed ICAL detector [3]. These cosmic muons act as a huge unwanted background interfering with the detection of muons arising from neutrino interactions. Placing a neutrino detector under a rock cover of 1km in all directions reduces the cosmic muon flux by a factor of $\sim 10^6$. At a depth of ~ 100 m or so, muons will be suppressed by a factor of $\sim 10^2$. To achieve a reduction factor 10^6, an active CMV system with an efficiency of $\geq 99.99\%$ must be built around such a shallow depth detector

to veto events arising from cosmic ray muons. The prototype detector of the ICAL i.e., mini-ICAL is currently in operation at IICHEP, Madurai [4]. The mini-ICAL consists of wenty $2\,m \times 2\,m$ glass RPCs sandwiched between 11 layers of 5.6 cm thick soft iron plates in the central $2\,m \times 4\,m$ region. The detector is magnetised using two sets of copper coils of 18 turns each. The central region of the mini-ICAL, where the RPCs are placed, has a nearly uniform magnetic field of 1.4 T for a coil current of $\sim$ 900 amps. To suppress the cosmic muon background, it is planned is to cover the top and three sides of the mini-ICAL with an active veto detector for the detection of the cosmic ray muons and estimate the CMV efficiency of the detector, using the same concept as the Mu2e collaboration [5]. The goal is to build an active veto detector with an efficiency of 99.99% and a false-positive rate of less than 10^{-5}.

The CMV detector for mini-ICAL will have four layers of extruded scintillators [6] of size 450 cm $\times$ 5 cm $\times$ 2 cm on top and three layers of 460 cm $\times$ 5 cm $\times$ 1 cm on three sides of the mini-ICAL [7]. The fourth side is planned to not be covered with veto layers due to the maintenance and troubleshooting of the mini-ICAL. In all, the veto system will comprise more than 700 extruded plastic scintillators. The surface area of each layer on top is $(450\,cm \times 440\,cm)$ and is $(460\,cm \times 200\,cm)$ for each of the side layers. The scintillation signal will be collected through WLS fibres [8] embedded in the extruded scintillator and the light from both ends of the fibres will be readout using SiPMs.

This paper describes the test setup to characterise $\sim$ 3500 SiPMs. These studies were performed as a part of the R&D program for the CMV system around mini-ICAL. Along with the basic performance studies we have also looked in detail at the effect of temperature on the SiPM and whether a feedback circuit is required for V_{bias} to compensate for the gain of SiPM due to the variation of temperature or not.

2 Hamamatsu SiPM 13360-2050VE

The SiPM selected for the CMVD experiment is the Hamamatsu S13360-2050VE. This SiPM model has an effective photosensitive area of 2 mm$\times$2 mm and a total of 1584 square microcells with a microcell pitch of 50 μm, fill factor of 74%, the breakdown voltage of (53 $\pm$ 5) V at room temperature [9]. The 2 mm$\times$2 mm active area of the chosen SiPM (S13360-2050VE) makes it very suitable for coupling with the WLS fibre of 1.4 mm diameter. The SiPMs are available mounted on tiny Carrier Boards (sim-like structure on left in figure 1) and 16 such carrier boards are present in a panel as shown on the right in figure 1.

3 Test Setup for mass testing of the SiPMs

The major components used for SiPM testing are LED driver as a light source, DRS for front end readout, and Transimpedance (TI) amplifiers to amplify the raw SiPM signals. Before going to the overall setup, here are some of the details about these major components.

3.1 Pulsed LED for characterising the SiPMs

The standalone SiPMs were tested and characterised using an SP5601 CAEN LED system [10]. The LED system consists of an ultrafast LED driver with tunable periodicity and

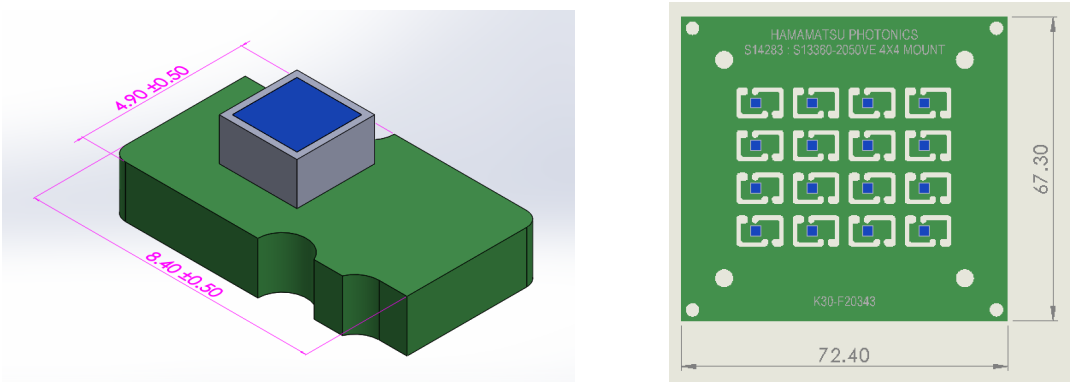

Figure 1: Geometrical structure of 16 SiPMs in a panel on right, sim like structure of a SiPM on left.

intensity and a pulse width of a few ns. It can provide a light burst with a tunable intensity varying from a few to more than tens of photons required for calibration purposes.

3.2 DRS4

The Domino Ring Sampler (DRS4) ASIC is a switched capacitor array (SCA) capable of sampling 9 differential input channels at a sampling speed of up to 5 GS/s [11]. The SCA consists of 1024 capacitive cells per channel to store the input analog waveform. The stored waveform samples can be readout via a shift register clocked at 33 MHz for external digitization. For SIPM data collection we used the DRS4 evaluation board [12]. The evaluation board has four analog inputs, a USB connection for data readout and board configuration and, on-board trigger logic. It is equivalent to a four channel 5 GS/s digital oscilloscope. The Evaluation boards come with PC software to display the waveforms captured from the four-input channels as well as store the captured data in the local disc.

3.3 Transimpedance Amplifier

The SIPM generates a charge of around 0.27 pC for every photoelectron (p.e.) at V_{ov} of 2.5 V. The current that flows due to this charge into a 50 Ω termination resistor of an oscilloscope, generates a very small voltage pulse of the order of a few millivolts. To get reliable charge distribution data, a Trans-Impedance (TI) amplifier was used. The gain of the TI amplifier is determined by the collector resistor, RA1 in parallel combination with RE1 shown in figure 2. The OpAmp stage provides a further gain of 1.37 and helps in driving the coaxial cable.

3.4 Overall Setup

A wooden black box of size 120 cm×60 cm was used for mass testing of the SiPMs with the LED source. The overall setup is shown in figure 3. The test setup contains a motherboard to mount the 16 SiPM's panel (figure 1) which was fixed inside the black box. The SiPMs on the panel will have secure electrical connections using pogo (spring-loaded) pins on the motherboard. The LED driver is kept inside the black box such that the SiPM will directly

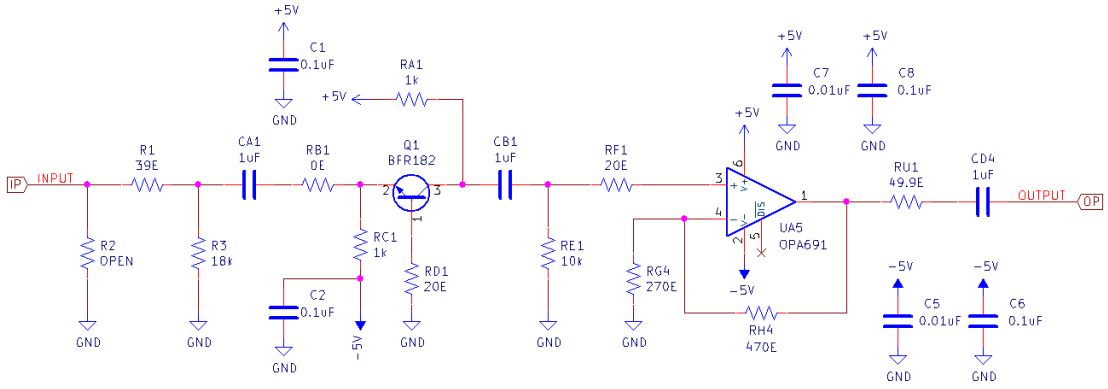

Figure 2: Circuit for the Transimpedance Amplifier.

face the LED flash. The LED pulse is synchronized with a trigger by an external pulser. A Tyvek paper was used as a screen between the LED driver and the SiPMs to diffuse the light. The intensity of the LED source and the distance from the SiPMs is adjusted so that a handful of photons are incident on every SiPM and the charge distribution can be seen clearly without saturating the system.

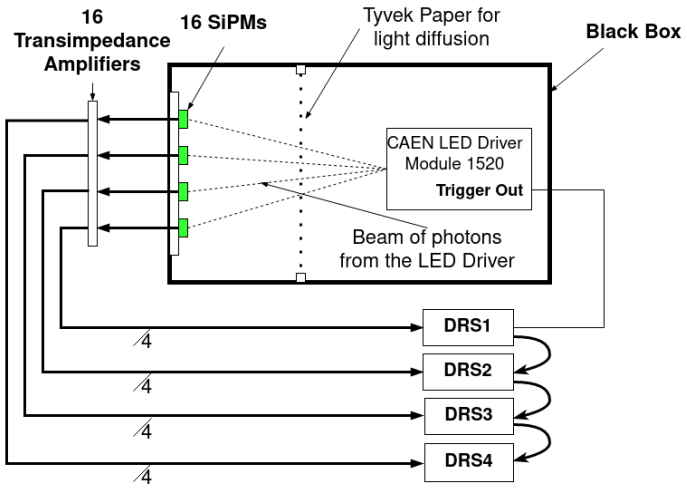

Figure 3: Signal readout paths through the DRS system.

When photons from the LED are incident on the SiPMs, electron-hole pairs will be generated in the corresponding microcells and an avalanche will be produced in every corresponding microcell due to the applied bias voltage (V_{bias}) leading to a current pulse in the circuit. For analog SiPMs (common readout for all microcells), the overall signal of the SiPM will be proportional to the number of individual microcell signals which are read. The SiPM signals are taken from the motherboard to the TI amplifiers using coaxial cables, the voltage signals (amplified SiPM signals) of the TI amplifiers are then connected to the DRS

waveform sampler modules as it is shown in figure 4. The LED driver generates a trigger pulse when it fires the LEDs, this signal was used as a trigger input to the DRS modules, 4 of which were used to capture the signals of the 16 SiPMs. The charge generated by every SiPM was measured from the DRS data by using the equation 3.1

$$q = \frac{1}{R \times G} \int_{to}^{t1} V(t)dt \tag{3.1}$$

where R is the input resistance of the transimpedance amplifier and G is the gain of the operational amplifier stage.

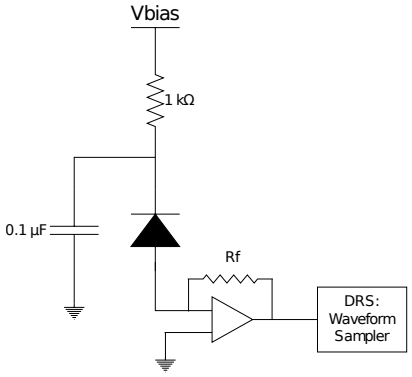

Figure 4: Schematic diagram of SiPM test setup.

4 Data Analysis

As discussed in the section 3, there are 16 SiPMs carrier boards in one panel, and all those 16 SiPM are illuminated with LED at the same time and each of the SiPM signals is amplified by a TI amplifier of gain 0.909 mV/μA and the output voltage is stored through the DRS system. The sampling rate is 2 GHz. Typical signals of SiPM are shown in figure 5. The first signal figure 5(a) is the clean output correlated with the LED pulse. The rise time of the pulse is ∼6 ns and the signal falls with a decay constant of ∼28 ns. The rise time of SiPM pulse without an amplifier is ∼2 ns, increase of rising time to 6 ns is due to the effect of the TI amplifier, whereas the decay constant mainly depends on the quenching resistance and associated capacitances. Signals in figure 5(b) and 5(c) shows the LED signal associated with single and double p.e. peaks due to single dark noise and two dark noise events respectively. The LED signal may also be associated with signals from optical cross talk, as shown in figure 5(d). The dark noise and optical crosstalk depend on the temperature and V_{ov} [7].

A SiPM is characterised by its gain as a function of V_{ov}, its dependence on temperature and noise rate as a function of V_{ov} and temperature. The gain of a SiPM is defined as the integrated charge due to a single p.e. as defined in equation 3.1. The integration time is taken as 100 ns, which contains more than 95% of the signal. This optimum width is chosen to reduce the dark noise as well as accept most of the signal. The signals in figure 5

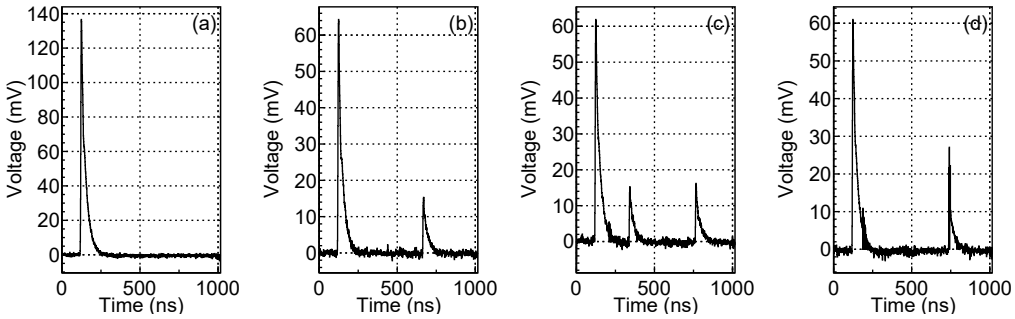

Figure 5: Raw signals of SiPM; (a) Ideal clear signal of LED, (b) signal with one dark noise, (c) signal with two dark noises and (d) signal with optical crosstalk signal.

show the baseline of the electronic signal to be close to zero, but to avoid any baseline fluctuations, integrated pedestal values of the same 100 ns width is subtracted from the signal. Typical integrated signals due to LED exposure are shown in figure 6(a) for two SiPMs on a single panel. From this figure, it is clear that the gain of different SiPMs is not exactly the same, although the specifications are the same. The gain is quantified by fitting those distributions with the combination of Gaussian functions for each p.e. peak and a wider background function. A typical fit is shown in figure 6(b). Details of the fit function are given in [7]. As different peaks are due to different p.e., the gap between two peaks is the estimation of the gain of the SiPM at that V_{ov} and the temperature.

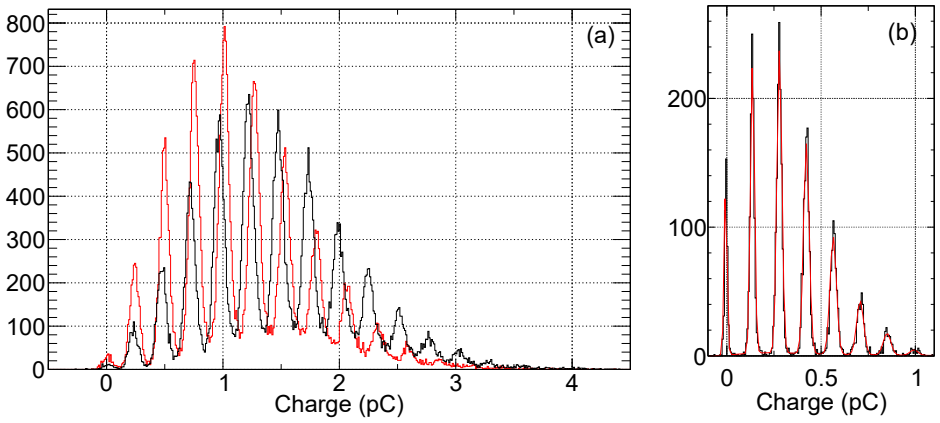

Figure 6: Pedestal subtracted integrated signals due to LED pulse at at 54 V for (a) two SiPM in a panel and (b) Fit of a spectrum to obtain gain.

To obtain the threshold voltage (V_{th}) and the variation of gain with respect to applied HV (dG/dV) data are collected for five different HV above the rated V_{th}. A typical distribution of gain vs HV is shown in figure 7. The points are fitted with a simple linear function, where the intercept of the line in the voltage axis is defined as V_{th} and the slope, (dG/dV) is the measure of the variation of gain with the change in overvoltage, V_{ov}, the difference between the V_{bias} and V_{th}. During this data taking, the temperature was not controlled properly, but the room temperature was 24±1° C. The effect of temperature will

be discussed in detail in section 6.

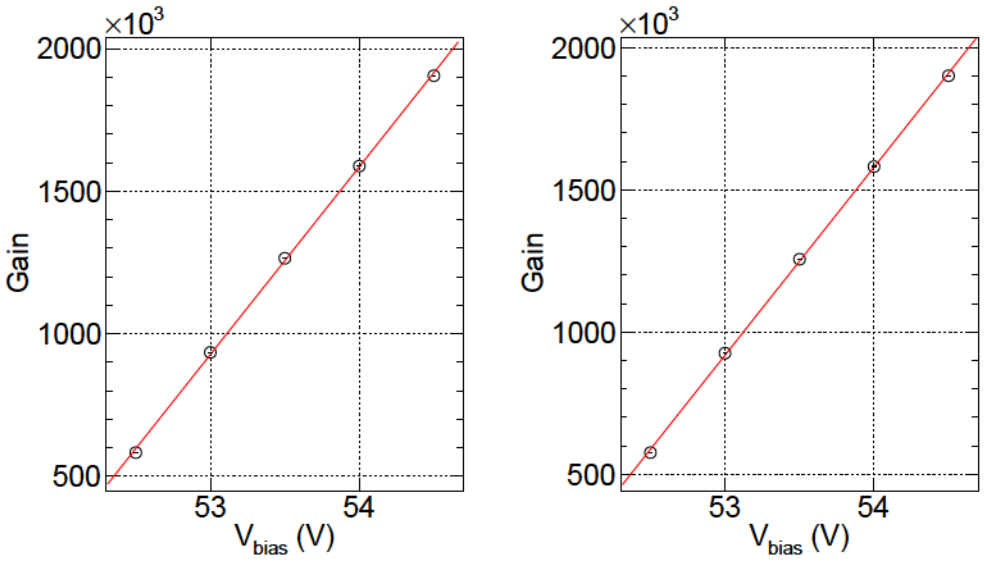

Figure 7: Variation of gain as a function of applied HV along with the linear fit function for few SiPMs.

There were a total of 220 panels with 16 SiPMs each. The SiPMs of one of the panels were used before the testing, thus we have tested all the SiPMs in the remaining 219 panels. The V_{th} of all SiPMs are shown in figure 8. The V_{th} varies from 50.7 V to 52.3 V and matches with the specification given by Hamamatsu, at 25 °C. The point to mention is that the V_{th} of SiPMs in each panel are nearly the same and the maximum deviation is 0.5 V.

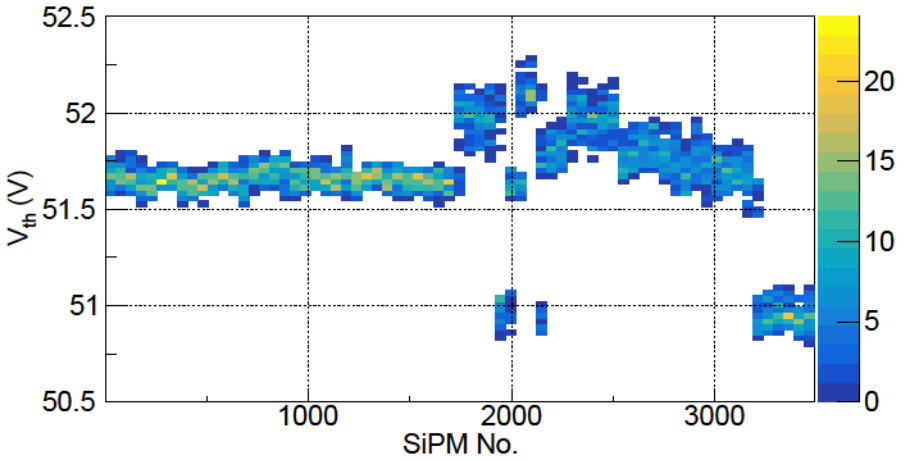

Figure 8: V_{th} of all tested SiPMs for CMVD.

The variation of gain with respect to applied voltage (dG/dV) about the V_{th} is shown in figure 9. Most of the SiPMs are having $dG/dV \sim 6.8 \times 10^5$. There are few outliers, but only one SiPM has much lower gain, 5.1×10^5.

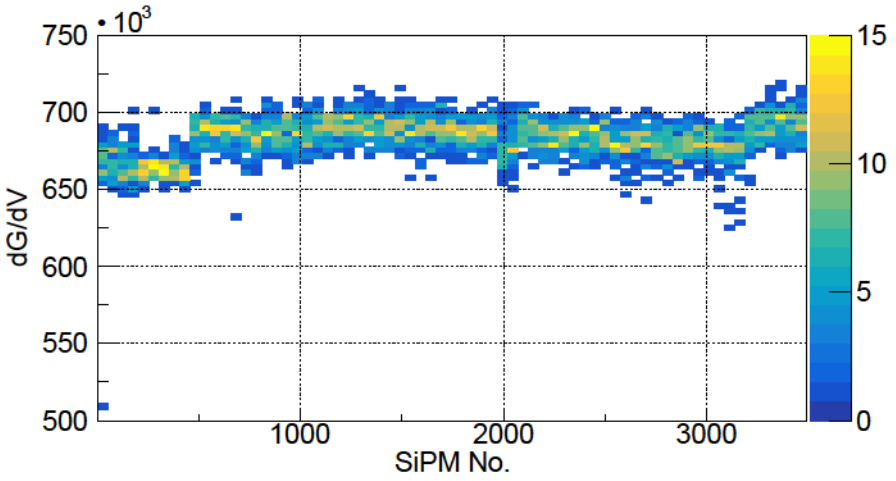

Figure 9: dG/dV of all tested SiPMs for CMVD.

From the figures 8 and 9 it is clear that all except one SiPM (low gain with $dG/dV \sim 5.1 \times 10^5$) is suitable for the CMV, where gains in all SiPMs are reasonably high and the variation of V_{th} is moderate. The third crucial parameter of the SiPM is dark noise. That was estimated by integrating the SiPM signal by randomly triggered 100 ns time windows. All these data were taken without any LED source and also at $V_{th} \sim 3$ V. The random noise is calculated by counting the fraction of events with an integrated signal more than 0.48 pC, which is equivalent to ~ 1.5 p.e.. The variation of noise rate for all these SiPM is shown in figure 10. The maximum noise rate at 1.5 p.e. threshold is 34.9 kHz for V_{th}=3 V, which is well below the acceptance threshold [7].

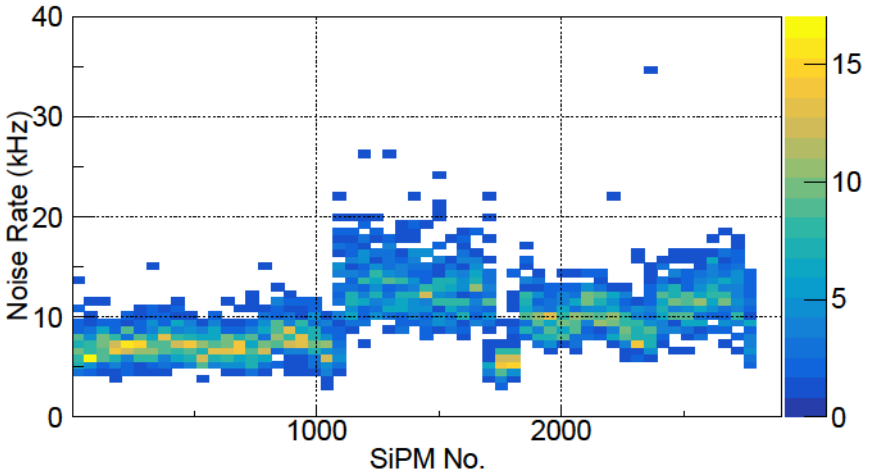

Figure 10: Noise rate of all tested SiPM for V_{ov} 3 V and Q_{th} 0.48 pC.

Based on the criteria and the noise rate of individual SiPM, all SiPM are satisfying the requirements of the CMVD. The figure 11 shows the correlation of noise rate with dG/dV on left and V_{th} on right respectively. There is no observed correlation of noise with those

two parameters.

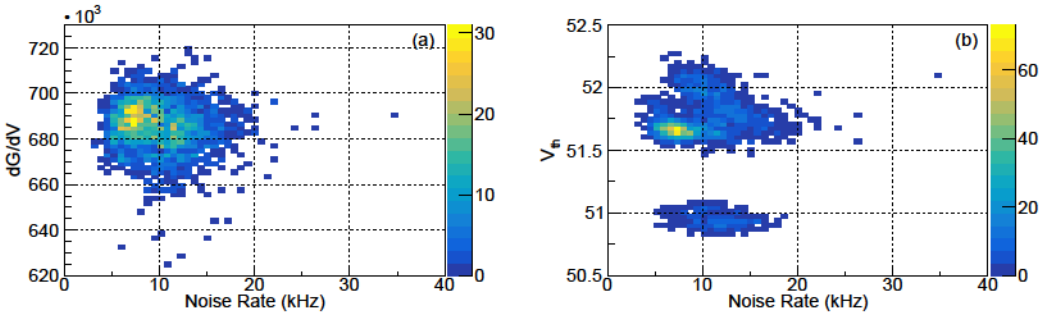

Figure 11: Correlation between the noise rate and a) dG/dV, b) V_{th}.

5 Setup for Controlled Temperature Testing

SiPMs show a large variation of their gain on the operational temperature. As per the SiPM datasheet, the temperature coefficient of the operating voltage is 54 mV/° C. To measure this value, it was necessary to take the setup shown in the figure 3 above to a chamber where the temperature could be maintained at a known value. We used the thermal chamber, "SU-642" from "ESPEC" for this purpose. A view of our set up inside the chamber is shown in figure 12. This chamber can maintain a temperature from −20 to 80° C with a temperature fluctuation of ±0.3° C [13], but during the data taking period, the temperature is varied from −20 to 50° C.

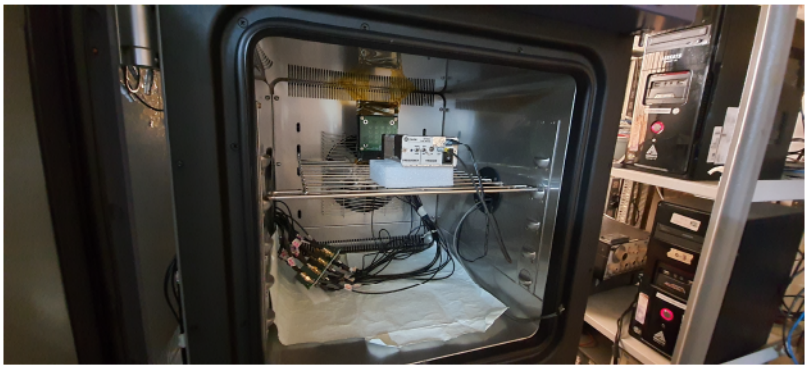

Figure 12: Setup inside controlled temperature chamber.

6 Variation of the gain of SiPM with temperature

For this study, we have used only 4 SiPMs of one panel. The temperature of the chamber is varied from −20° C to +50° C and for each temperature, LED data are taken for around 20 voltages. There are many data points around 25° C, which is the average operating temperature in the IICHEP laboratory.

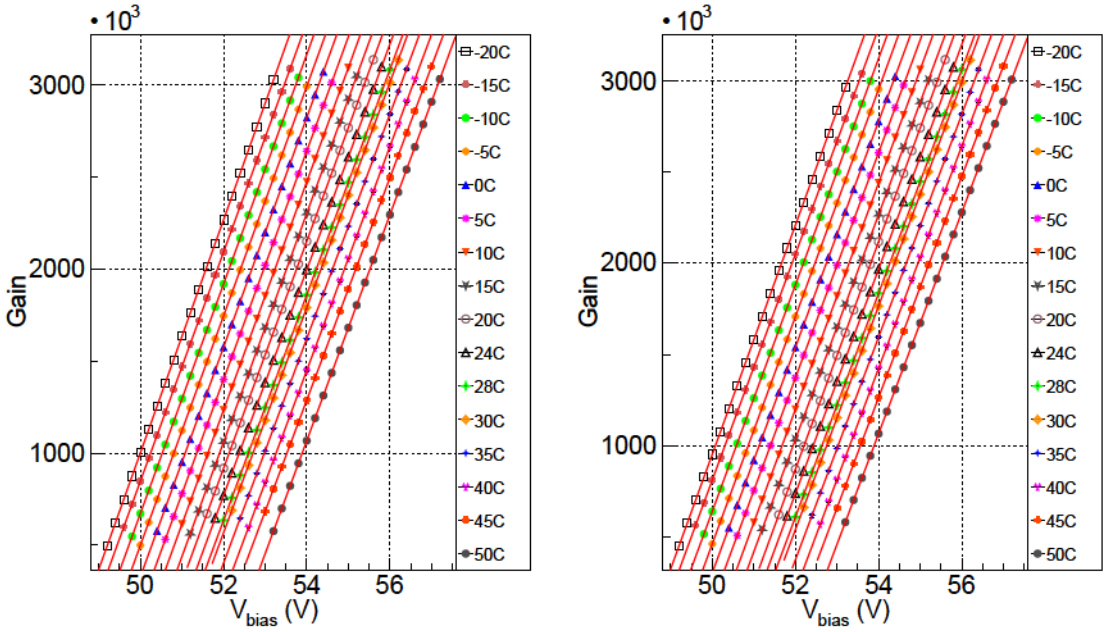

Figure 13: The gain versus applied voltage for various temperatures for two SiPMs.

The variations of absolute gain as a function of applied voltage are shown in figure 13 for different temperatures. The gain of SiPM is varying linearly with increasing applied voltage and hence is fitted with a linear function for estimating the variation of gain with respect to the applied voltage (dG/dV) and threshold voltage (V_{th}) at each temperature. The variations of the observed V_{th} as a function of temperature are shown in figure 14 along with a linear fit to estimate the variation of V_{th} with respect to temperature (dV_{th}/dT) for two of the SiPMs. The observed values of dV_{th}/dT for tested SiPMs are consistent with the value given in specifications [9].

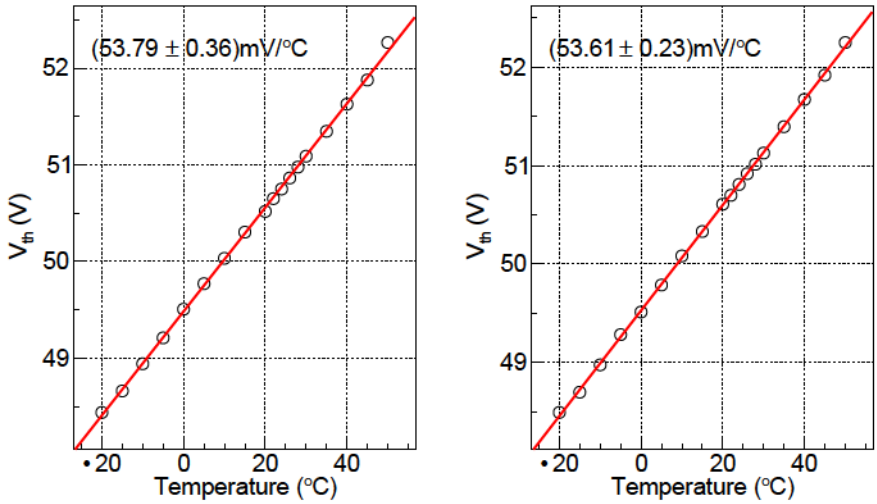

Figure 14: Variation of V_{th} with temperature for the same 2 SiPMs.

The observed slopes (dG/dV) from the linear fit in figure 13 at different temperatures are shown in figure 15 for few SiPMs. These plots show the decrease of dG/dV with temperature. The behaviour has been seen in literature [14, 15].

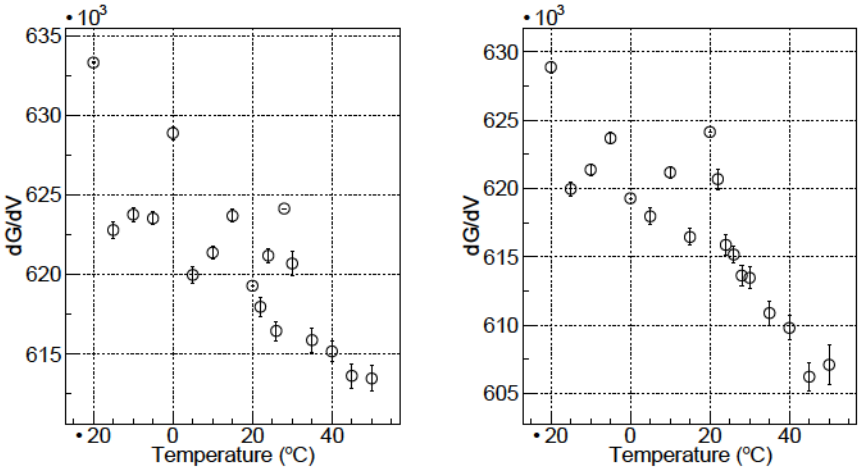

Figure 15: dG/dV versus temperature for two of the SiPMs.

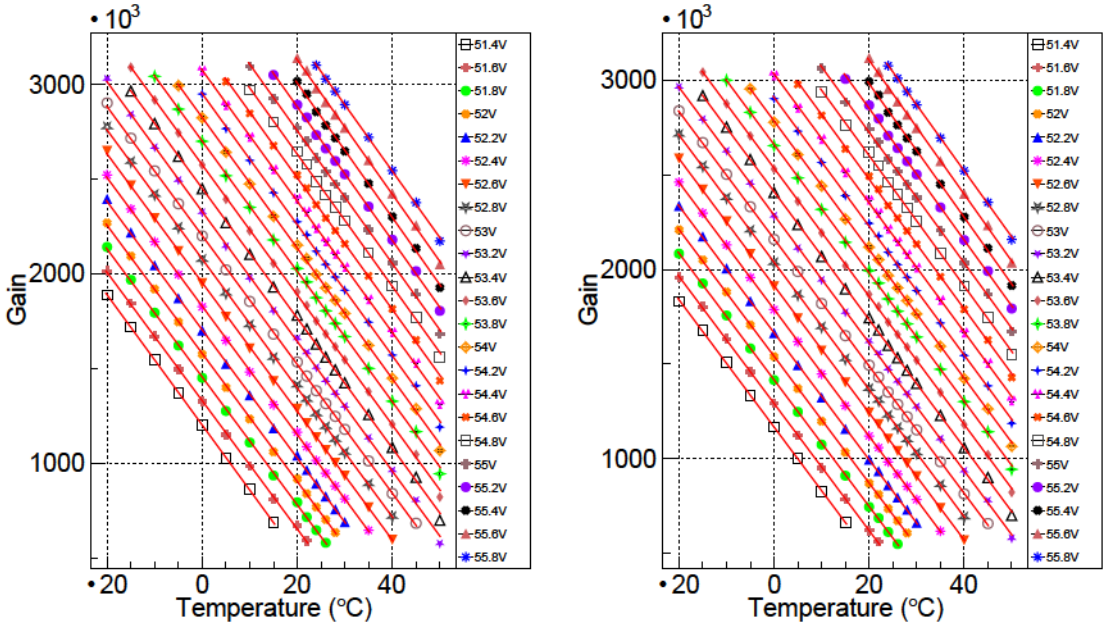

Figure 16: The gain versus temperature for various applied voltages for the two SiPMs.

The variations of absolute gain as a function of temperature are shown in figure 16 for different applied voltages. As expected the gain is higher at lower temperatures, which is mainly due to the shift of V_{ov}. For each applied voltage the gain is fitted with a linear function and the observed slopes (dG/dT) for these two SiPMs are shown in figure 17. The magnitude of dG/dT varies with the applied voltage, which indicates a variation of dG/dV for different temperatures.

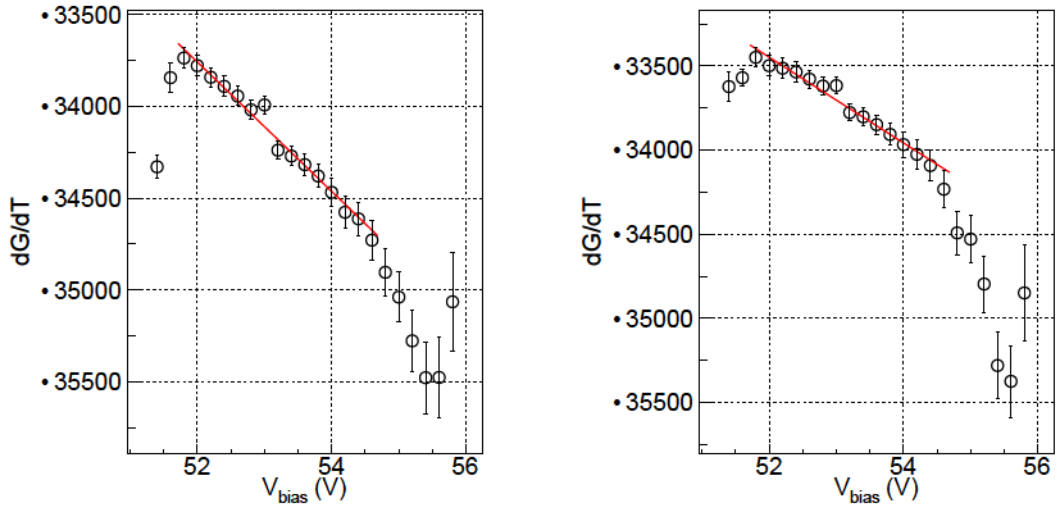

Figure 17: dG/dT versus applied voltage for two SiPMs.

Using the slopes dG/dV and dG/dT, dV/dT is estimated. The average value of dG/dT is evaluated using the values of dG/dT in linear range from figure 17. The ratio of average value of dG/dT to dG/dV at a given temperature is used to calculate dV/dT at that particular temperature. The variations in dV/dT are shown in figure 18 as a function of temperature, where the value varies from (53.5 - 55.5) mV/° C.

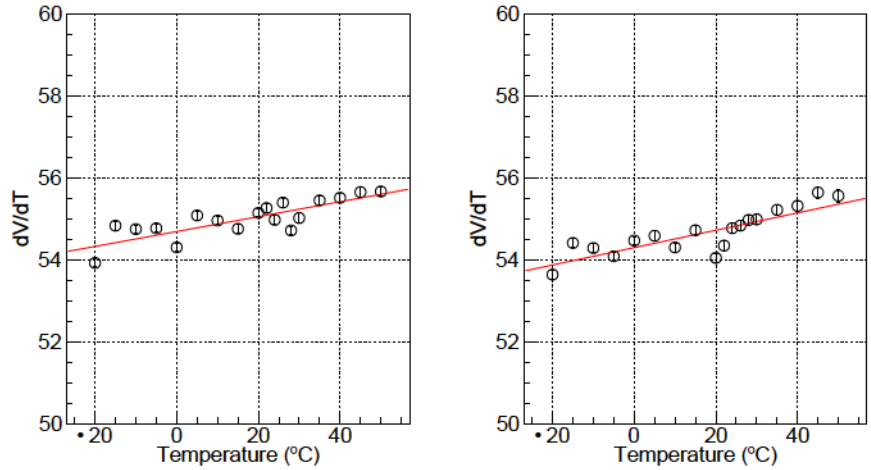

Figure 18: dV/dT versus T for two of the SiPMs.

7 The effect on efficiency and noise rate with the change in V_{ov}

There is no extra control of temperature in the CMVD electronics, other than the default control through the room air conditioning system in the mini-ICAL room, where the variation of temperature is about 2° C. The gain of the SiPM decreases with increasing temperature because V_{th} shifts toward the higher side. The change in gain of SiPM with

temperature will have an impact on the efficiency and the noise rate of the CMVD. To compensate for the gain change due to temperature change, the bias to the SiPM needs to be adjusted. As it can be observed in figure 18, average value of dV/dT is $\sim$55 mV/° C. This implies that the change in operating voltage would be $\sim$110 mV. Do we need a feedback system in the SiPM power supply to compensate for the variation of temperature for the CMVD requirement, i.e. the efficiency of the veto wall should be more than 99.99% with the range of temperature variation, and similarly the ratio of the fake to true muon rate should be less than 10^{-5} ? The randomly/noise triggered data and the cosmic muon triggered data have been collected at V_{ov} of 2.5 V $\pm$ 200 mV at room temperature, whereas 2.5 V is optimised value of V_{ov} for CMVD operation [7]. A total of 13 sets of data are collected to see the effect of gain change of SiPM (w.r.t. applied voltage change) on the CMVD performance.

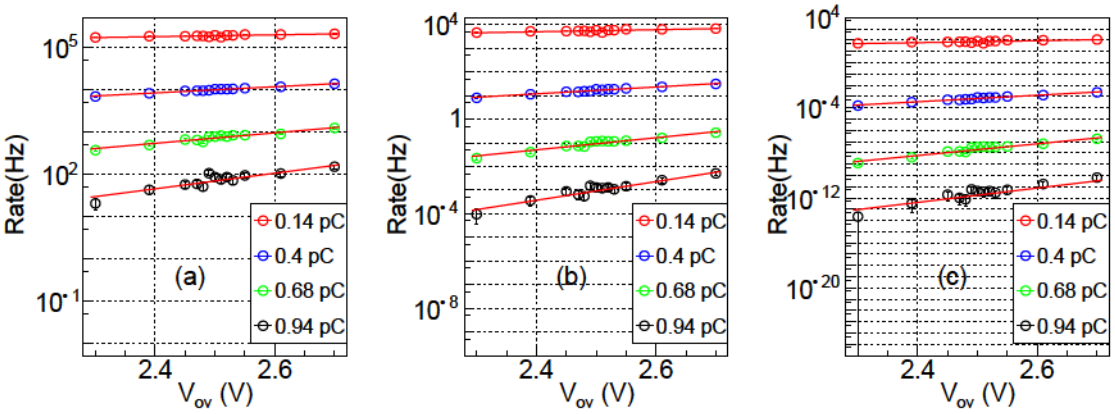

Figure 19: The noise rate as a function of V_{ov} and q_{th} of (a) an individual SiPM, (b) a scintillator where at least two out of four SiPMs will have signal and (c) of CMVD for atleast two out of four layers satisfy trigger criteria when at least two out of four SiPMs will have signal in a scintillator.

From the noise data, the individual noise rates of 4 SiPMs are calculated as a function of V_{ov} and q_{th} and is shown in figure 19(a) for one the SiPMs. Using the individual noise rates of 4 SiPMs, the noise rate of a scintillator is estimated when at least two out of four SiPMs have a signal and then these noise rates are propagated to estimate the noise rate of CMVD for any two out of four-layer trigger criterion as a function of V_{ov} and q_{th} and the rates are shown in figure 19(b) and figure 19(c) respectively. At the chosen q_{th}=0.68 pC which is equivalent to 2.5 p.e. for V_{ov}=2.5 V, for CMVD operation, the noise rate of CMVD for the highest value of V_{ov} (i.e. 2.7 V) is $\sim 10^{-7}$ Hz. The cosmic muon signal will be integrated within a 100 ns during CMVD operation. The noise rate at q_{th}=0.68 pC for a 100 ns window will be $\sim 10^{-14}$ Hz which is well below the tolerable noise rate for CMVD requirement [7].

For the efficiency measurement of a complete scintillator of length 4.7 m, the scintillator is equipped with WLS fibre and SiPMs are mounted on both sides to collect the signal and measure the efficiency of the cosmic muon, which are triggered by three similar scintillator

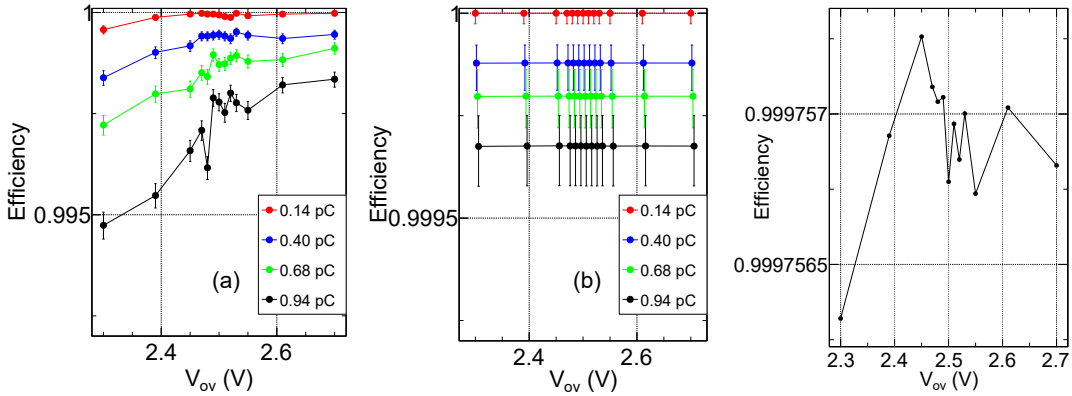

Figure 20: The muon detection efficiency of (a) an individual SiPM as a function of V_{ov} and q_{th}, (b) a scintillator as a function of V_{ov} and q_{th} when at least two out of four SiPMs will have signal and (c) a scintillator for q_{th}=0.68 pC, the error on the data points in last plot is less than 10^{-4}.

detectors. The applied voltage of the SiPMs is varied up to ±200 mV about the V_{ov}= 2.5 V and the variation in the efficiency of SiPM and the scintillator detector is checked and then extrapolated to the efficiency of the four-layer veto wall as described in [7].

The cosmic muon efficiency is measured for individual SiPMs as shown in figure 20(a) as a function of V_{ov} and q_{th}. Also, the cosmic muon efficiency is measured when atleast two out of four SiPMs will have signal and it is shown in figure 20(b) as a function of V_{ov} and q_{th}. Figure 20(c) shows the cosmic muon efficiency of a scintillator as a function of V_{ov} at q_{th}=0.68 pC, this plot shows the statistical fluctuations in efficiency for different V_{ov} which can't be seen in figure 20(b) due to the efficiency scale. The scintillator efficiency at the lowest value of V_{ov} i.e. 2.3 V, is high enough to attain the efficiency requirements for the CMVD operation [7].

This study concludes that even if V_{ov} is not compensated for ± 4° C variation at IICHEP lab, CMVD requirements will still be satisfied. Thus, neither it require a special temperature control on top of the air conditioning system nor a feedback option to change the operating voltage.

8 Summary

The main goal of this study is to test all SiPMs for the CMVD. The test results based on the gain and noise study show that all except one SiPM are acceptable for the CMVD. The variation in the threshold voltage of SiPM with temperature is studied and is found to be (53.5 - 54.5) mV/° C. The CMVD will be operated in an air-conditioned room, where the maximum variation in temperature is 2° C. Thus, a detailed study was done to find the variation in gain of SiPM as a function of temperature, which is found to be less than 2%/° C. This study also confirms that even with this variation of temperature, the performance of the CMVD detector will satisfy the design goal. The feedback electronic

circuit will not be required to change the operating voltage to compensate for the variation of SiPM gain due to the variation in temperature.

9 Acknowledgments

We sincerely thank Prof. Varsha R Chitnis, Mano Ranjan, S.R. Joshi, Darshana Gonji, Santosh Chavan, Vishal Asgolkar for their support and help during the work. We would also like to thank all other members of the INO collaboration for their valuable inputs.

References

[1] INO Project Report, 2006, www.ino.tifr.res.in/ino/.

[2] S. Ahmed, et al., *Physics Potential of the ICAL detector at the India-based Neutrino Observatory (INO)*, arXiv:1505.07380.

[3] L.N. Bogdanova, M.G. Gavrilov, V.N. Kornoukhov and A.S. Starostin, *Cosmic muon flux at shallow depths underground*, Physics of Atomic Nuclei 69 (2006) 1293-1298.

[4] Gobinda Majumder, et al., *Design, construction and performance of magnetised mini-ICAL detector module*, ICHEP 2019.

[5] Mu2e collaboration, R.J. Abrams et al., *Mu2e conceptual design report*, arXiv:1211.7019.

[6] Anna Pla-Dalmau, Alan D. Bross* and Kerry L. Mellott, *Low-cost extruded plastic scintillator*, Nuclear Instruments and Methods in Physics Research A 466 (2001) 482-491.

[7] Mamta Jangra, et al., *Characterization of Silicon-Photomultipliers for a Cosmic Muon Veto detector. Journal of Instrumentation*, 10.1088/1748-0221/16/11/P11029 **16** (2021) P11029.

[8] Kuraray Co., Ltd, http://kuraraypsf.jp/psf/.

[9] HAMAMATSU MPPC (Multi-Pixel Photon Counter) datasheet, https://www.hamamatsu.com/eu/en/product/type/S13360-2050VE/index.html

[10] SP5601 LED Driver, https://www.caen.it/products/sp5601.

[11] S. Ritt, *9 Channel, 5 GSPS Switched Capacitor Array*, https://www.psi.ch/sites/default/files/2020-08.

[12] DRS4, *DRS4 Evaluation Board User's Manual*, https://www.psi.ch/sites/default/files/2020-02.

[13] SU-642 specs, https://www.espec.co.jp/english/products/catalog/sh.

[14] Gerald Eigen, *Gain Stablization of SiPMs*, arXiv:1710.01648.

[15] Gerald Eigen, *SiPM Gain Stabilization Studies for Adaptive Power Supply*,arXiv:1603.00016.